A&A 397, 1151–1159 (2003)
DOI: 10.1051/0004-6361:20021559
© ESO 2003

Astronomy & Astrophysics

Precise radial velocity measurements of G and K giants⋆

First results

J. Setiawan[1], L. Pasquini[2], L. da Silva[3], O. von der Lühe[1], and A. Hatzes[4]

[1] Kiepenheuer-Institut für Sonnenphysik, Freiburg(Brsg), Germany
[2] European Southern Observatory, Garching bei München, Germany
[3] Observatório Nacional, Rio de Janeiro, Brazil
[4] Thüringer Landessternwarte Tautenburg, Tautenburg, Germany

Received 14 December 2001 / Accepted 25 October 2002

Abstract. We present the first results of our precise radial velocity (*RV*) measurements of G and K giants. A number of stars from our list of 80 targets have been observed for 14 months using the fibre-fed echelle spectrograph FEROS at the 1.52 m ESO telescope in La Silla, Chile. This sample increases the number of giants surveyed with precise stellar radial velocity measurements at least by a factor of 10. During this period we are able to estimate the long-term accuracy of our measurement as better than 11 m s^{-1}. We use the simultaneous Th-Ar calibration and cross-correlation technique to compute the radial velocity by applying a numerical template for K-type stars. Standard deviation σ of mean radial velocity variations between 3 m s^{-1} and 4 km s^{-1} with timescales between several days and years are measured for 21 of G and K giants which are presented in this paper. Fifteen stars show definite variability above 3 σ of our measurement uncertainties. Two stars with *RV* variations above 800 m s^{-1} are tentatively identified as new binaries. Although definitive trends between *RV* variations and stellar evolutionary status cannot yet be established, all the luminous cool giants of our sample seem to have significant radial velocity variations, while those stars in the giant's clump region can be either variable or constant.

Key words. stars: late-type – stars: variables: general – techniques: radial velocities

1. Introduction

Techniques for the measurement of precise stellar radial velocities were originally developed for the detection of extrasolar planets (Campbell & Walker 1979) and these have had spectacular success (Mayor & Queloz 1995; Marcy & Butler 1996). These kinds of measurements have also made important contribution to stellar physics by discovering new classes of variable stars. One such class of objects are the K giant stars. *RV* variability in the K giant Arcturus was first reported by Smith et al. (1987) using *RV* measurements taken with a Fabry Perot. Walker et al. (1989) then reported low-amplitude variability (30–300 m s^{-1}) in a sample of 6 cool giants. Subsequent *RV* studies established that K giant variability occurs on two timescales: 2–10 days (Smith et al. 1987; Hatzes & Cochran 1994, 1996) and several hundreds of days (Hatzes & Cochran 1993, 1999; Larson et al. 1993).

Photometric surveys of larger sample of giant stars have firmly established that variability of cool giants is indeed pervasive. Edmonds & Gilliland (1996) found variability with periods of 2–4 days and amplitudes of 5–15 mmag among K giants in the 47 Tuc cluster. Jorissen et al. (1997) found in a sample of 50 G–M giants that the minimum level of variability increased from KIII to mid-M spectral types. In the most extensive photometric survey Henry et al. (2000) found that in a sample of 187 G–M giants 43% of these were variable on timescales of days to weeks.

It is clear that the short-period variability are due to radial and/or nonradial pulsations. *RV* measurements have revealed up to 10 pulsation modes in Arcturus that are equally spaced in frequency, the characteristic signature of p-mode oscillations (Merline 1997; Hatzes & Cochran 1999). This star also shows long-period *RV* variations of 233 and 40 days (Hatzes & Cochran 1993). An extensive photometric study of the K giant α UMa using the Wide Field Infrared Explorer revealed 10 frequencies that were consistent with the stellar parameters for this star (Buzasi et al. 2000).

The large number of short-period pulsation modes found for a few cool giant stars suggests that these objects are amenable to asteroseismic studies. These can help determine such fundamental stellar parameters as the mass and radius,

Send offprint requests to: J. Setiawan,
e-mail: setiawan@kis.uni-freiburg.de

⋆ Based on observations collected at the ESO 1.52 m telescope at the La Silla Observatory under program ESO No. 64.L-0047, 65.L-0571, 66.D-0592 and from Nov. 99 to Feb. 01 under the ESO-Observatório Nacional, Brazil, agreement.

Article published by EDP Sciences and available at http://www.aanda.org or http://dx.doi.org/10.1051/0004-6361:20021559

as well as to probe the internal structure of the star. The latter is important for directly testing the predictions of stellar evolution theory. These asteroseismic studies are particularly important as the G–K giant stars occupy a region of the H–R diagram where the evolutionary tracks of a wide range of spectral types (A–G) converge. It is difficult to obtain accurate masses or to know the spectral type of the progenitor star. Asteroseismic studies can provide the crucial data for understanding these stars *if* we can find periods to the variations. Oscillations of short periods have been derived for only a few G–K giant stars, so it is not known how the oscillations change as a star evolves up the giant branch.

The nature of the long-period *RV* variations ($P > 100$ days) is still not yet completely understood and viable hypotheses include low-mass companions, rotational modulation by surface features, or non-radial pulsations. Arguments in favor of the companion hypothesis include the stability of the *RV* variations (Hatzes & Cochran 1993) and the lack of spectral variability in at least one K giant (Hatzes & Cochran 1998). Two candidates of extra-solar planets have been detected on K giants HD 27442 (Butler et al. 2001) and ι-Draconis (HD 137759) (Frink et al. 2002). The companion around ι-Draconis has a minimum mass of 8.9 $M_{\rm Jupiter}$ and a corresponding semi-major axis of 1.3 AU. Frink et al. (2002) also assumed an upper limit of 45 $M_{\rm Jupiter}$ using the non-detection of an orbit by HIPPARCOS to obtain the lower limit of the inclination. This implicates that the mass of the companion is below the hydrogen burning limit.

Arguments in favor of rotational modulation are based on the equivalent width variations of activity indicators for a few K giants (Larson et al. 1993; Lambert 1987). So far, the number of K giants for which long periods have been derived are too few to aid in discriminating between these various hypotheses.

In order to increase our knowledge about the long- and short-period variability in G and K giants, we began a survey of these stars spanning the entire Red Giant Branch (RGB) using precise *RV* measurements. This survey has several goals: 1) to find how the short-period variations behave as a star moves up the RGB, 2) to derive periods for the short-period variations that could be used for asteroseismic studies, 3) to discern the nature of the long-period variations. If indeed these variations are due to stellar surface structure, then our survey would provide targets for the VLTI, since many of these objects have large enough angular diameters to be resolved by this instrument. Here we present the preliminary results of our survey. We demonstrate that FEROS is capable of achieving the needed precision as better than 11 m s^{-1}. We also show that many of the cool giant stars in our sample show peak-to-peak *RV* variations of several hundreds of m s^{-1}, consistent with previous surveys.

2. Observations

From 1999 October 22nd to 2000 December 21st 39 nights were allocated to this program using FEROS, the echelle spectrograph at the 1.52 m ESO telescope in La Silla. Over 39 spectral orders, this instrument provides a full wavelength coverage between 3500 to 9200 Å at a resolving power $\lambda/\Delta\lambda$ of 48 000 (Kaufer & Pasquini 1998). This enabled us to record

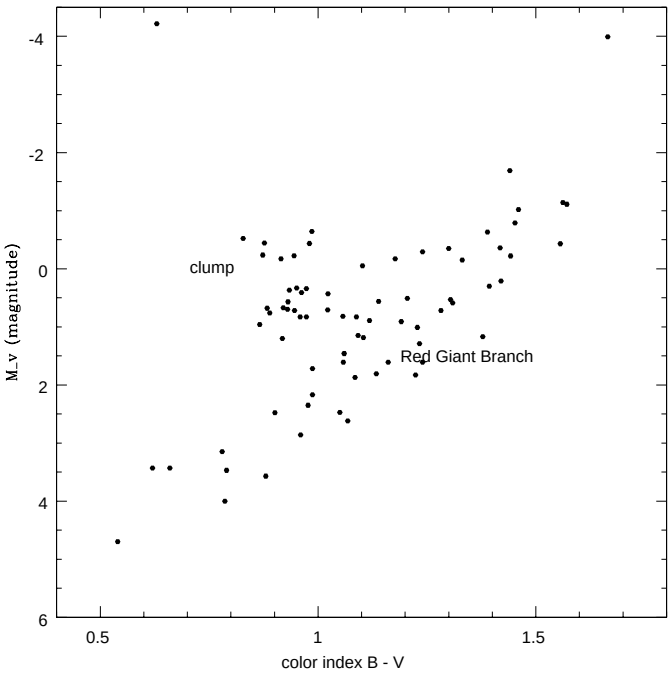

Fig. 1. H–R diagram of the target stars observed in our precise *RV* survey with FEROS. The sample covers the RGB including the "clump" region.

simultaneously to the portion of the spectrum used for accurate *RV* determinations such chromospheric activity indicators as Ca II H and K lines.

FEROS is equipped with a double fibre system, one for the object and a second fibre that can record sky or obtain a simultaneous wavelength calibration to be used for the accurate *RV* determination following the technique pioneered by the Geneva Observatory (see e.g. Baranne et al. 1996). An *RV* measurement error of 23 m s^{-1} was achieved in the commissioning period (Kaufer & Pasquini 1998) which was decreased to 10 m s^{-1} using an improved data reduction method (Setiawan et al. 2000). The program started with 27 stars in October 1999, but was expanded to 80 G and K giants after 14 months. The whole sample stars cover a large fraction of the upper H–R diagram including the full RGB as well as the "clump" region (see Fig. 1). To help in the reliable determination of stellar parameters the targets were selected on the basis of accurate HIPPARCOS parallaxes.

In the calibration session, a series of 2–5 Th-Ar exposures (*double Th-Ar*) were taken at the beginning, middle, and end of the night. To assess the quality of our *RV* measurements we also observed a "constant" (i.e. standard) star. We chose HD 10700 (τ-Ceti, spectral type G8V, $m_V = 3.50$) as our standard since it has measured *RV* variations less than 5 m s^{-1} (Butler et al. 1996); in addition it is also conveniently placed for observations at La Silla and very bright. We took additional Th-Ar calibration spectra just before the standard star observations to correct the FEROS systematic errors as discussed in the Sect. 4. During a full observing night, 30 to 40 science stellar spectra with exposure times varying from 2 min for of $m_V \simeq 2$ up to 30 min for fainter ones of $m_V \simeq 7$ were collected.

Being interested in abundances, Ca II variability, and bisector variations, we require an average signal to noise ratio (S/N) of about 150–200 per pixel. We found that this high S/N is appropriate for investigating variations of the Ca II K (λ3933). Since this is also the first precise *RV* study with FEROS, we wanted to be sure that the S/N of the observations was not our limiting factor.

The data were first processed at the telescope immediately after observations using the FEROS reduction pipeline. This was used primarily as a "quick look" to ensure the quality of the data.

3. Data analysis

Our *RV* analysis required two main steps: the data reduction with the ESO-MIDAS and the cross-correlation with a proper numerical template (*mask*). The data reduction was performed using the FEROS context in the MIDAS environment, but not using the pipeline results. The extracted and wavelength calibrated spectra were not merged in a single spectrum, rather 39 separate spectra (one/order) were produced for each fibre spectrum. To compute the radial velocities, cross-correlation functions (CCF) were performed by using the TACOS package, developed by the Geneva Observatory. The cross-correlation mask used for all stellar observations is one appropriate for a K-type dwarf. The long term stability of the Th-Ar calibration has been monitored and the instrumental drifts have been corrected by using cross-correlations of the calibration exposures with a thorium mask (see Baranne et al. 1996 for details). The stellar mask covers a wavelength region from 3900–6997 Å. The data reduction and cross-correlation processes are described in more detail in the following subsections.

3.1. Data reduction in the ESO-MIDAS environment

The reduction of science frames consisted of the standard steps of bias subtraction, bad column correction, order extraction, division by a flat field, wavelength calibration and correction for the barycentric velocity. For the order extraction we used the extraction mode with rejection of cosmics ray events. This was prefered to the widely used "optimal extraction" (Horne 1986) to minimize the handling of the original data and the risk of introducing spurious effects. We also note that at the S/N ratio of our observations, the difference in the final S/N ratio between the two extraction methods is minimal. The blaze correction was done by dividing the extracted spectra by the average flat field, which is created by using the calibrations obtained in the same night. After the spectral extraction a linear rebinning was performed in 0.03 Å steps order by order.

We did not find it necessary to change the default values for the the wavelength calibration parameters set in FEROS context, while several modifications to the original MIDAS commands were required with respect to rebinning of the spectra: 1) the barycentric correction was computed using the middle exposure time rather than the start exposure time, 2) the barycentric correction was not applied to the second fibre, in which the simultaneous Th-Ar is taken, but only to the first fibre (object fibre), 3) we used proper telescope and star coordinates, not taken directly from the observations FITS headers. While these details do not affect the general observer, they may be relevant when trying to achieve an accuracy of a few m s^{-1}.

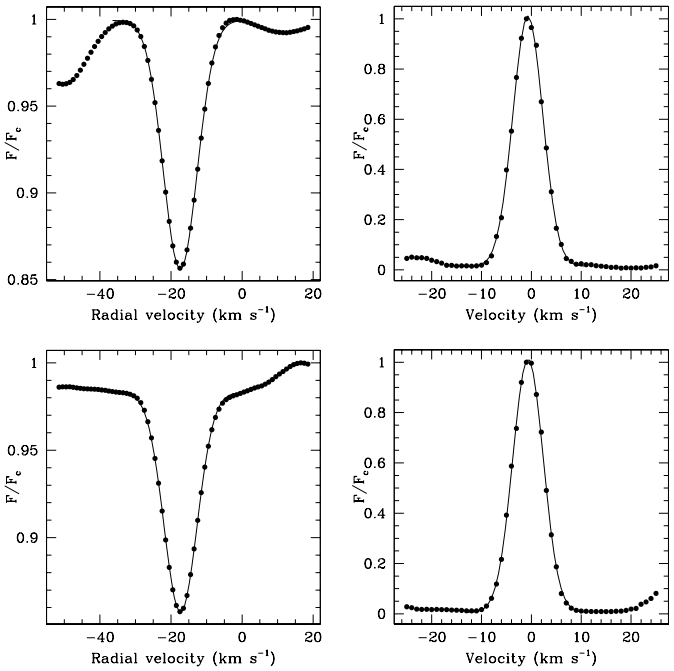

Fig. 2. Cross-correlation functions (CCF) of two orders (upper row: order 21 and lower row: order 24) which are well fitted with the Gaussian. Figures in the left column demonstrate the CCF of the stellar absorption spectra (here: our standard star τ-Ceti) with the stellar mask, whereas figures in the right column show the CCF of the Th-Ar calibration emission spectra with the thorium mask.

3.2. Radial velocity computation

The *RV* computation was carried out using the TACOS cross-correlation routines, which operated on one dimensional order spectra with an appropriate numerical template, e.g. stellar mask for fibre 1, thorium mask for fibre 2 as well as for double Th-Ar exposures. The resulting CCF was fitted with a Gaussian. Since the thorium mask needs to be adapted to each spectrograph, we modified the original thorium mask (provided by the Geneva Observatory, built for ELODIE) by checking the CCF profile every 10 Å steps over the region from 3700–7200 Å. Mask positions which correspond to wavelength region containing strong/broad lines in the spectra were taken out, because they introduced spurious noise into the Gaussian fit or resulted in the disappearance of the CCF. After this process we therefore had a proper thorium mask for FEROS. We remark that in the data reduction the true echelle orders 102–63 were renumbered from 1–39. However, since the stellar mask ends at 6997 Å, only the data reduction orders 7–31 covering the wavelength region 3910–6997 Å were used for the *RV* computation.

From the maximum position of the Gaussian we obtain the position of the maximum in the CCF used for the *RV* determination. The width of the Gaussian $\sigma_{\rm CCF}$ can be used to compute the projected rotational velocity $v \sin i$ as done in Queloz et al. (1998). However, we would like to discuss this somewhere else.

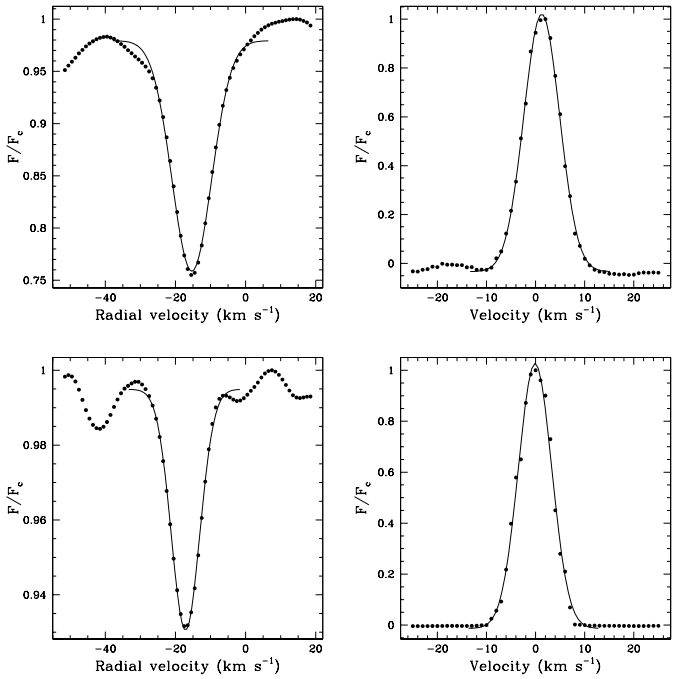

Fig. 3. CCF of two orders, also computed for τ-Ceti (upper row: order 7 and lower row: order 31). The two orders demonstrate the worst fits with the Gaussian.

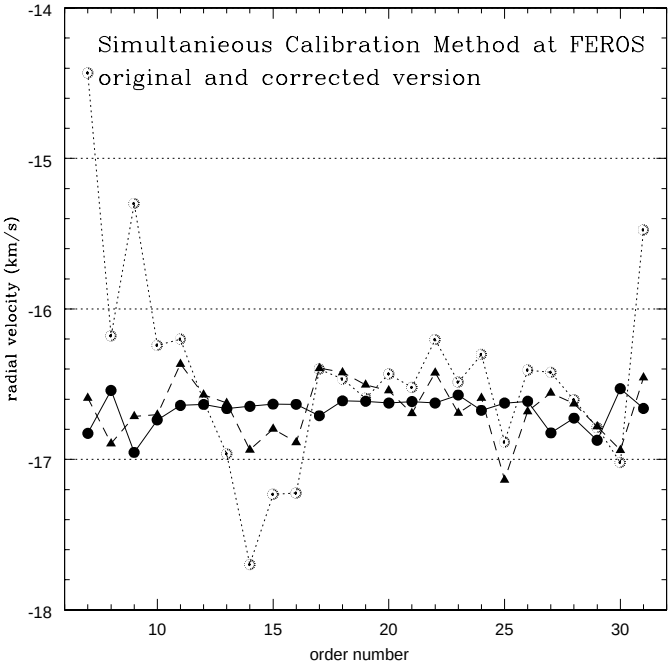

Fig. 4. A comparison between the original simultaneous calibration (open circle connected by dot-line) and the corrected version: 1. triangles connected by dashed line: applying the double Th-Ar correction as given in Eqs. (2)–(3), 2. full filled circles connected by solid lines: the double Th-Ar correction and the order-offset correction as given in Eqs. (4)–(9).

In Figs. 2 and 3 we show some CCF profiles of our standard star τ-Ceti, which has a stable *RV*. Examples of excellent Gaussian fits (order 21 and 24) to the CCF are shown in Fig. 2. Poorly Gaussian fits (e.g. order 7 and 31) are shown in Fig. 3.

The method to compute the *RV* of each spectrum, which was developed for use with data from CORAVEL, ELODIE and CORALIE, is given by the equation:

$$RV = \frac{1}{N}\sum_i (\mathrm{O}_i - \mathrm{C}_i), \tag{1}$$

where i is the order number, N is the total number of orders used, O is the *RV* for the object fibre and C for the simultaneous calibration. We modified this equation slightly as given in the Sect. 4 to correct the FEROS systematic errors. Mean *RV* were computed using both an unweighted mean as well as a mean weighted by the rms of the individual order. No noticeable improvement in the *RV* was found when using the weighted mean. We however observed a systematic error as dependence of the mean *RV* for each order of the standard star τ-Ceti when averaging over many spectra. This pattern can be explained by systematic zero-point shifts of the stellar spectrum template used in the cross-correlation.

4. Obtaining the FEROS accuracy and error analysis

When determining the long-term spectrograph accuracy we experienced some difficulities in the spectrograph performance in that the simultaneous Th-Ar spectra did not provide adequate zero-offsets. Thus, subtracting the *RV* of fibre 2 (simultaneous Th-Ar) from fibre 1 (object) as given in the Eq. (1) still left residual velocity errors of up to 100 m s^{-1} over the course of one year of observing. One way to correct this systematic error is to use the double Th-Ar exposures after applying the data reduction procedures for science exposures to them. The double Th-Ar calibration residual velocities were subtracted from the original *RV* computation.

$$RV = \frac{1}{N}\sum_i (\mathrm{O}_i - \mathrm{C}_i - T_i), \tag{2}$$

where T_i is a correction factor determined by:

$$T_i = \mathrm{ThAr1}_i - \mathrm{ThAr2}_i \tag{3}$$

ThAr1 and ThAr2 were taken from the double Th-Ar exposures (fibre 1 and fibre 2). This correction is a very efficient way to eliminate the largest noise contributions came from orders in the red region (order 31, center wavelength λ_c = 6855 Å), in the blue region (order 7 to 10, λ = 3890–4270 Å) and order 14 (λ_c = 4525 Å) as demonstrated in Fig. 4. It was therefore necessary always to take double Th-Ar exposures and to build a new wavelength solution directly before taking the standard star exposure. This method was quite successful in reducing the systematic error. We estimate a long-term accuracy, given by the standard deviation σ as better than 11 m s^{-1} when comparing *RV* measurements of individual stars over about one year. By rejecting 3 data points (2 from June 2000 and 1 from November 2000) we obtain a standard deviation of 10.1 m s^{-1} for our standard star τ-Ceti. The 3 measurements (open circles in Fig. 5), which deviate more than 60 m s^{-1}, are suspected as results of uncorrected calibration (the Th-Ar spectra are too weak due to a problem with a mirror in the FEROS calibration unit). Even if

we take these 3 measurements into account, we still achieve a σ of 15.5 m s^{-1}. Although still an excellent precision, σ is at least a factor of 3 worse than the known *RV* stability of the star. The slightly poorer *RV* precision is possibly associated with using a numerical template which is appropriate for a K0 dwarf and not the hotter G dwarf. We therefore might be able to achieve a better *RV* precision on τ-Ceti using a template that is more appropriate for this star. We also cannot exclude uncorrected systematic errors due to features peculiar to FEROS that are not found in CORALIE and ELODIE which achieve a better *RV* precision. These include the use of an image slicer or the absence of a double fibre scrambler.

To correct the order-offsets we computed the mean *RV* of the 25 orders separately by using 63 spectra of one year observation of τ-Ceti (Fig. 6a). Figure 6b shows the order dispersion σ_e, given by $\sigma/\sqrt{N-1}$, where N is the total number of spectra. Orders 11 through 29, except 14 and 15, have σ_e less than 15 m s^{-1}, some orders have σ_e less than 10 m s^{-1}. The largest noise contributions come from orders in the red region (order 30 and 31), as well in the blue region (order 7 to 10). Since the mean *RV* of each orders are largely separated up to 1 km s^{-1} (see Fig. 6c), a simple averaging of 25 *RV* values will result in errors of about 50 m s^{-1} for each spectrum. Thus we applied an order-offset correction for τ-Ceti as outlined below.

First, we computed the *RV* mean value of each order from all spectra obtained.

$$RV_i = \frac{1}{N} \sum_{j=1,..,N} RV_{i,j}, \tag{4}$$

where $i = 7, .., 31$ is the order number, j is the spectrum sequence number and N is the total number of spectra. Then we build the mean *RV* of the 25 orders used:

$$\overline{RV} = \frac{1}{25} \sum_{i=7,..,31} RV_i. \tag{5}$$

The offset of each order δ_i is given by

$$\delta_i = RV_i - \overline{RV}. \tag{6}$$

Using the notation *RVC* for corrected *RV*, we applied these offsets to every single *RV* computation:

$$RVC_{i,j} = RV_{i,j} - \delta_i. \tag{7}$$

The mean radial velocity of the jth spectrum is

$$\overline{RVC}_j = \frac{1}{25} \sum_{i=7,..,31} RVC_{i,j}, \tag{8}$$

and finaly, we obtain the corrected mean *RV* of the total N spectra taken during the whole observation:

$$RV_{\rm mean} = \frac{1}{N} \sum_{j=1,..,N} \overline{RVC}_j. \tag{9}$$

The long-term FEROS accuracy is determined by the standard deviation σ of $RV_{\rm mean}$ of the standard star. We applied the τ-Ceti's order-offsets to the other spectra of each star and successfully reduced the error down to 20 m s^{-1}. We note that the profile of the *RV* variation does not change when applying this order-offsets correction.

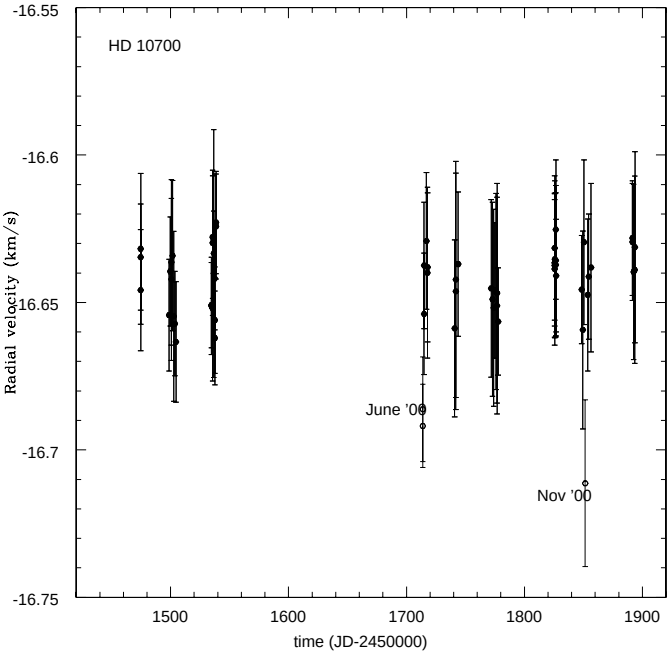

Fig. 5. The *RV* measurements of τ-Ceti taken with FEROS spanning one year. The rms scatter of all the data points is 15.5 m s^{-1}. By neglecting the three data points represented by open circles the sigma is reduced to 10.1 m s^{-1}.

We may still improve this result by investigating, in case that these offsets are not optimized for other stellar spectra. Our goal is to reach the 10 m s^{-1} accuracy of each spectrum, as it has been shown when determining σ_e of each order. This improvement is still possible because τ-Ceti has a different spectral type than the majority of our targets.

5. Results

Although our final sample has been expanded after 14 months from a size of 27 to 80 giants, only a few program stars have more than 20 observations which is adequate for assessing the *RV* stability of the star. In Table 1 we present the *RV* results for 22 stars sorted by their standard deviation σ. With respect to the σ values we classify our results in four categories as described below. A sample of the *RV* plot for each class is given in Fig. 7a–7d. We classify a star as variable if it has a standard deviation in the *RV* larger than 30 m s^{-1}, that is approximatively three times the FEROS accuracy found for τ-Ceti, or if a periodogram for this star shows significant power at a certain period.

1. Stars which show no significant *RV* variation (σ < 20 m s^{-1}: HD 36189 (Fig. 7a), HD 16147, as well as our standard star τ-Ceti (HD 10700).
2. σ between 20 m s^{-1} and 30 m s^{-1} were obtained for HD 18322, HD 18885 (Fig. 7b), HD 36462, and HD 36848. Since this is less than 3 times of the FEROS accuracy, it is difficult to verify if these stars are indeed variable.

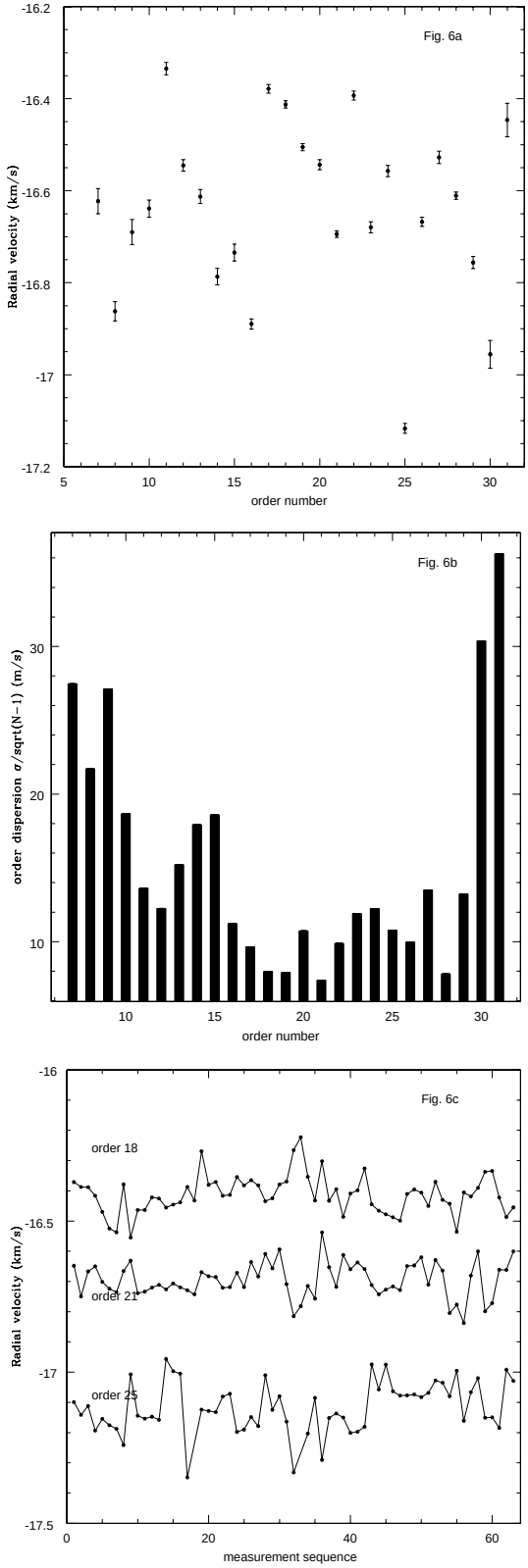

Fig. 6. Figure 6a shows the mean values of measured *RV* variations obtained from 63 spectra of τ-Ceti for individual orders. The error bars are the standard error of the mean $\sigma_e = \sigma/\sqrt{N-1}$. Figure 6b shows the σ_e of the 25 cross-dispersed echelle orders (order 7–31). Figure 6c shows order dependence of the measured *RV* of τ-Ceti. The orders 18, 21, and 25 have standard errors σ_e of better than 15 m s^{-1}, but the "gaps" between them vary from 300 m s^{-1} (between order 18 and 21) to 700 m s^{-1} (between order 18 and 25).

Table 1. Radial velocity variations of 22 program stars and 5 stars of past observations, sorted after σ.

HD	Sp. type	M_V [mag]	$B-V$	σ[m s^{-1}]
36189	G6III	−0.64	0.99	2.62
10700	G8V	5.69	0.72	10.05
16417	G5IV	3.43	0.66	13.53
34642	K0IV	2.17	0.99	23.59
18885	G6III	1.15	1.09	25.94
18322	K1III	0.83	1.09	27.27
36848	K2III	1.83	1.22	29.82
62509[a]	K0III	1.08	1.00	31.42
11977	G8.5III	0.57	0.93	32.09
161096[b]	K1III	0.77	1.19	35.31
175751	K1III	0.82	1.06	36.07
12438	G5III	0.68	0.88	36.73
32887	K4III	−1.02	1.46	45.56
27256	G8II−III	0.92	0.91	46.92
152334	K4III	0.30	1.39	48.34
165760	G8III−IV	0.33	0.95	51.54
18907	G5IV	3.47	0.79	67.88
107446	K3/K4III	−0.63	1.39	70.52
124897[a]	K1.5III	−0.30	1.23	84.68
156283[c]	K3I	−2.09	1.46	104.23
224533	G9III	0.70	0.93	108.84
81797	K3III	−1.69	1.44	124.43
29139[a]	K5III	−0.65	1.54	127.49
50778	K4III	−0.36	1.42	134.88
179799	K0	2.35	0.98	682.58
22663	K1III	0.43	1.02	846.99
40176	K1III	−0.05	1.10	3210.01

[a] Hatzes & Cochran (1993).
[b] Hatzes & Cochran (1994).
[c] Hatzes & Cochran (1999).

3. σ between 30 and 100 m s^{-1} are obtained for HD 11977, HD 175751, HD 12438 (Fig. 7c), HD 32887, HD 27256, HD 152334, HD 165760, HD 18907, HD 107446. They may have *RV* amplitude variations between 50 m s^{-1} and 200 m s^{-1}. Those which also seem to have long-period oscillations are interesting for further investigation of low-mass companion.
4. *RV* variations with σ larger than 100 m s^{-1} were observed on the stars: HD 224533, HD 81797, HD 50778 (Fig. 7d), HD 179799, HD 22663 and HD 40176. HD 224533 and HD 179799 are cataloged as stars in double system or multiple system. Speckle observations of HD 224533 result an angular separation of 0.945 arcsec between the components (Horch et al. 1999). Further investigations are needed to establish if the variations are due to rotational modulation of surface structure or low-mass companions.

Table 1 shows that so far most of the stars have *RV* variation limited to ∼200 m s^{-1}, and only 3 stars are separated from the rest of the group. One is the multiple HD 179799, the other two are HD 22663 and HD 40176. The large amplitude of the *RV* variations, coupled with the fact that the stars do not occupy a

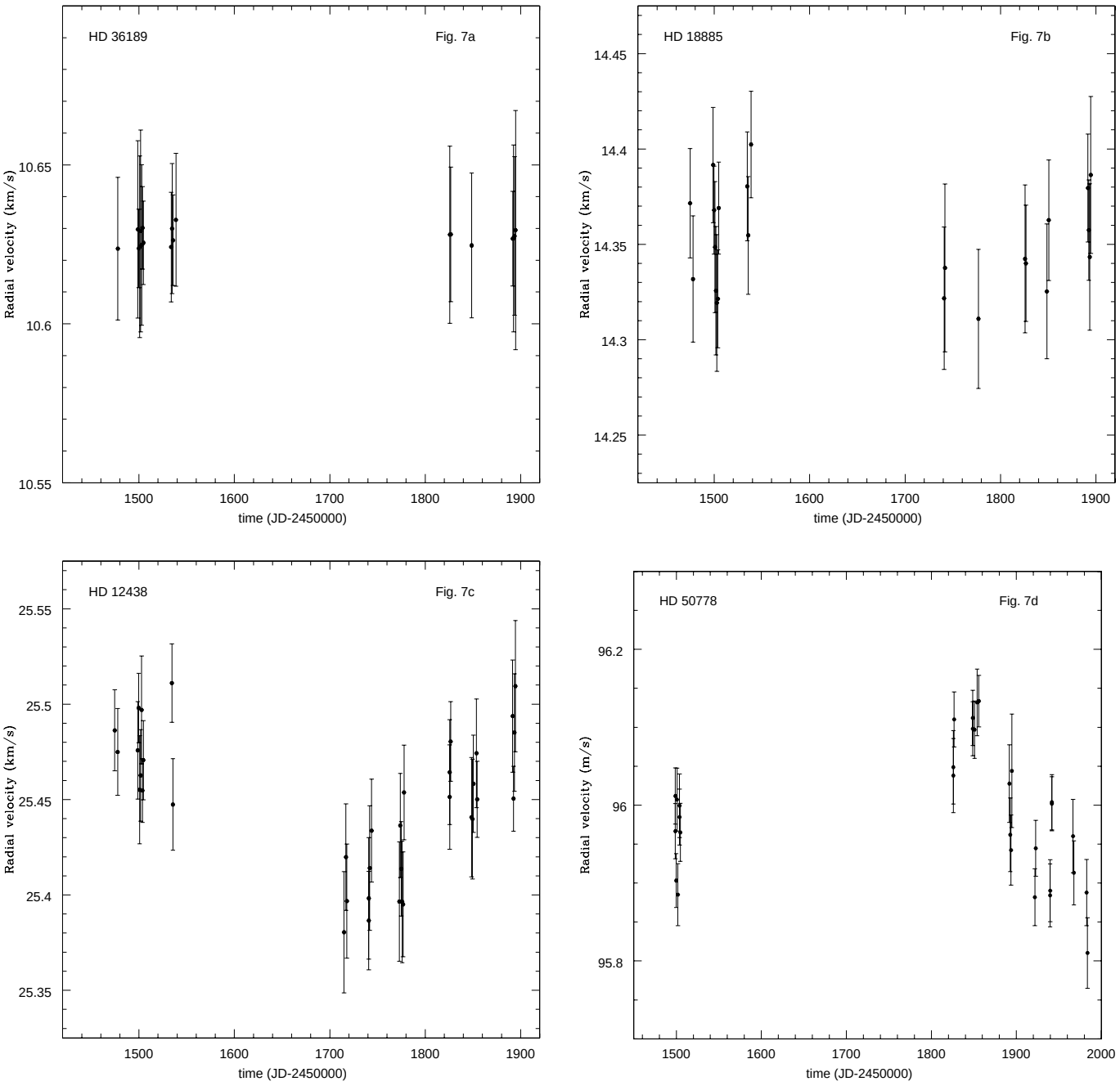

Fig. 7. Figures 7a–7d show type stars of each category discussed in Sect. 5. The dots are mean values of measured spectra consisting 25 echelle orders. The error bars represent the standard error of the mean value $\sigma_e = \sigma/\sqrt{N-1}$.

region of the H–R diagram known for strong variability leads us to suspect that HD 22663 and HD 40176 are single-lined spectroscopic binary stars since their σ exceed 800 m s^{-1}.

Figure 8 shows an H–R diagram with σ of each individual star presented by dots and circles. Our results show that there is a dependence of the *RV* variation with respect to position on the RGB. The open circles with solid line indicate known double stars. The dotted open circles are results of past observations (Hatzes & Cochran 1993, 1994, 1999). The size of the symbols corresponds to the σ-values, except those for binaries. The binaries are presented in a fixed scaling because of their large *RV* variations compared to single giants of our targets.

In the region of color index $1.4 < B - V < 1.5$ the σ values are between 60–150 m s^{-1}. In the clump region the major σ values are between 30–60 m s^{-1}, only the binaries show large variations with σ up to 3 km s^{-1}.

Considering mass companions as the source of *RV* variations it is still too early to conclude, given the short time span of our observations and the sampling, whether the *RV* variations result from companions around the main star. A comparison of the *RV* variation with the rotational velocity $v \sin i$ of the star and with stellar activity indicators (Ca II H and K lines) is required. We expect to improve our results after obtaining more observation data. Furthermore we will be able to complete the

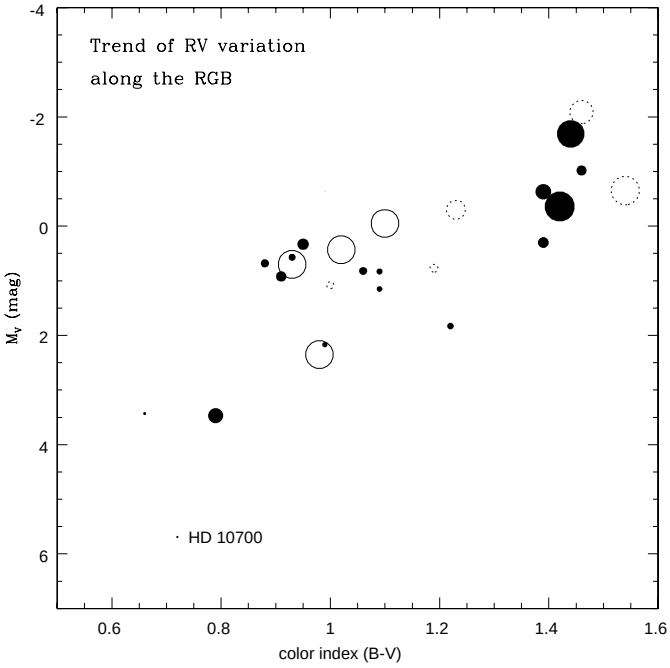

Fig. 8. H–R diagram of analyzed 22 stars and 5 stars from past observations. The size of the dots and circles represents the σ-values. The full dots are single giants of our targets, whereas the open circles indicate known double stars. The dotted open circles refer to past observations.

analysis of the other 58 stars and to compute their radial velocities in order to investigate any trend of *RV* variation along the RGB.

6. Discussion

Depending on the period, the *RV* variations in giant stars can be caused by either low-mass companions, oscillations, or rotationally induced variations from surface inhomogenities. Given a significant sample we might be able to distinguish between these hypothesis by investigating the behavior of the *RV* variations as a function of position along the H–R diagram. The presence of low-mass companions should not be a function of the stellar evolutionary status, whereas for the other two hypotheses we should expect a systematic change in the *RV* behavior as a function of evolutionary status. For example, the rotational period is expected to increase as the star evolves off the main sequence, although the evolution of the angular momentum may well depend on the stellar mass (Pasquini et al. 2000). If the *RV* variations were induced by inhomogenities present at the stellar surface we should expect some semi-regular pattern along the giant branch, with periods generally increasing with increasing colors. As far as amplitudes are concerned, it is not clear how they should vary with stellar effective temperature and luminosity, since variations will depend likely on the extension of the inhomogenities and their contrast with the underlying photosphere, and both quantities are largely unknown. However, in first approximation these amplitudes should be largely determined by the position of the star in the color-magnitude diagram, although some scatter should be definitely expected.

In the case of stellar oscillations, detailed models do not exist for stars very different from the Sun, however, by simply adopting reasonable scaling laws and assumptions, Kjedlsen & Bedding (1995) showed that solar-type oscillations amplitudes should change smoothly along the color magnitude diagram, scaling essentially as L/M. Although field stars of different masses can partially overlap in the H–R diagram, we again expect to see some regular pattern among our targets, if the *RV* variations were induced by solar-type oscillations. The region where some larger variations could be expected is the region around the "clump", because, while this region is dominated by He-core burning phase of relatively massive stars, due to uncertainties in the measurements and to difference in metallicities, some stars in these region could be low-mass metal poor in RGB phase. The structural parameters of the stars should therefore be different and some large scatter in the amplitude and general behaviour of stars around the clump region could be observed. We note, in passing, that if we assume that the chromosphere is a good tracer of the external layers of giant stars, Dupree et al. (1999) did not find large differences between M 67 clump and RGB stars having similar colors and temperatures, indicating that these deep structural differences may not be reflected in differences in the outer layers of the stars.

We find in our first result that HD 224533 has a low σ for a double star, which is less than 200 $\mathrm{m\,s^{-1}}$, but probably we have not covered the whole period yet. For this star a separation of 0.945 arcsec (Horch et al. 1999) and a difference in magnitude between the two components of 5.3 mag have been measured, which makes the secondary a main sequence star in the 0.8 $M_\odot$ range if at the same distance of the primary. With a stellar distance of 68.55 parsec, the separation between the components would be 64.7 AU. We assume a binary system with $m_1 = 2\,M_\odot$, $m_2 = 0.8\,M_\odot$ and the 64.7 AU separation as the semi-major axis of the orbit. Following the binary model we find an expected orbital period and semi-amplitude for this system of $P = 308.6$ years and $K_1 = 1778.6 \cdot \sin i / \sqrt{1-e^2}\ \mathrm{m\,s^{-1}}$. We observed a *RV* variation with a semi-amplitude of $K_1 < 1\ \mathrm{km\,s^{-1}}$. If the *RV* variation observed is caused by the visual companion mentioned above, we asumme that for a moderately orbital eccentricity, e.g. $e = 0.3$, we have to set an inclination $i = 28°$ to reconcile the inferred and the expected *RV* semi-amplitudes. However, it is still not clear if the *RV* variability observed within one year is indeed due to the companion with the expected periodicity of 308.6 years. It is also possible that this *RV* variation is not due to the visual companion but caused by another unseen companions.

7. Conclusion

We have reduced and analysed high resolution spectra for 22 giants over 14 months to investigate their *RV* variability. By using the G dwarf τ-Ceti as a calibrator we obtain an accuracy of as better than 11 $\mathrm{m\,s^{-1}}$ over this period. Out of the 21 G and K giants which we have analyzed, 15 (~75%) show definite *RV* variability at the 3 σ (30 $\mathrm{m\,s^{-1}}$) level. Although our results do not yet allow to establish firm trends between *RV*

variability and position of the stars in the H–R diagram, another significant effect seems to be that all luminous cool stars exhibit considerable *RV* variations.

In addition to the two stars (HD 224533 and HD 179799) which have previous indications of duplicity, we find evidence that 2 additional stars, HD 22663 and HD 40176, are also multiple systems. This is based on the fact that these stars show a very large *RV* amplitude (σ larger than 800 m s^{-1}).

Considering the system HD 224533, it is still unknown if the observed *RV* variation is caused by the visual companion or by another unseen companions.

Acknowledgements. We are grateful to A. Torrejon and R. Vega for their help in assisting during observations, and D. Queloz for many suggestions and for sharing experience with the TACOS software. L. da S. thanks the CNPq Brazilian Agency for the financial support through grant 200580/97.

References

Baranne, A., Queloz, D., Mayor, M., et al. 1996, A&AS, 119, 373
Butler, R. P., Marcy, G. W., Williams, E., et al. 1996, PASP, 108, 500
Butler, R. P., Tinney, C. G., Marcy, G. W., et al. 2001, ApJ, 555, 410
Buzasi, D., Catanzarite, J., Laher, R., et al. 2000, ApJ, 532, L133
Campbell, B., & Walker, G. A. H. 1979, PASP, 91, 540
Dupree, A. K., Whitney, B. A., & Pasquini, L. 1999, ApJ, 520, 751
Edmonds, P. D., & Gilliland, R. L. 1996, ApJ, 464, L157
Frink, S., Mitchell, D. S., Quirrenbach, A., et al. 2002, ApJ, 576, 478
Hatzes A. P., & Cochran, W. D. 1993, ApJ, 413, 339
Hatzes A. P., & Cochran, W. D. 1994, ApJ, 422, 366
Hatzes A. P., & Cochran, W. D. 1996, ApJ, 468, 391
Hatzes A. P., & Cochran, W. D. 1998, MNRAS, 293, 469
Hatzes A. P., & Cochran, W. D. 1999, MNRAS, 304, 109
Henry, G. W., Fekel, F. C., Henry, S. M., et al. 2000, ApJS, 130, 201
Horch, E., Ninkov, Z., van Altena, W. F., et al. 1999, AJ, 117, 548
Horne, K. 1986, PASP, 98, 609
Jorissen, A., Mowlavi, N., Sterken, C., et al. 1997, A&A, 324, 578
Kaufer, A., & Pasquini, L. 1998, SPIE, 3355, 844
Kjedlsen, H., & Bedding, T. R. 1995, A&A, 293, 87
Larson, A. M. Irwin, A. W., Yang, S. L. S., et al. 1993, PASP, 105, 332
Lambert, D. L. 1987, ApJS, 65, 255
Mayor, M., & Queloz, D. 1995, Nature, 378, 355
Marcy, G., & Butler, P. 1996, SPIE, 2704, 46
Merline, W. J. 1997, Ph.D. Thesis, The University of Arizona, Tucson, AZ
Pasquini, L., de Medeiros, J. R., & Girardi, L. 2000, A&A, 361, 1011
Queloz, D., Allain, S., Mermilliod, J. C., et al. 1998, A&A, 335, 183
Setiawan, J., Pasquini, L., da Silva, L., et al. 2000, The Messenger, 102
Smith, P. H., McMillan, R. S., & Merline, W. J. 1987, ApJ, 317, L79
Walker, G. A. H., Yang, S., Campbell, B., et al. 1989, ApJ, 343, L21